Comparison of cardiovascular parameter estimation methods using swine data

Comparison of cardiovascular parameter estimation methods using swine data

Cite this article as: Tatsuya Arai, Kichang Lee and Richard J. Cohen, Comparison of cardiovascular parameter estimation methods using swine data, Journal of Clinical Monitoring and Computing https://doi.org/10.1007/s10877-019-00322-y

Comparison of Cardiovascular Parameter Estimation Methods Using Swine Data

Tatsuya Arai[1], and Kichang Lee[2,3], Richard J. Cohen[2],

Department of Aeronautics and Astronautics[1] and Institute for Medical Engineering and Science[2]

Massachusetts Institute of Technology, Cambridge, MA 02139; the Cardiovascular Research Center[3],

Massachusetts General Hospital, Boston, MA 02114

Running head: Cardiovascular Parameter Estimation

Corresponding Author:

Kichang Lee, Ph.D.

Institute for Medical Engineering and Science

Massachusetts Institute of Technology

45 Carleton Street, Room E25-324

Cambridge, MA 02142

Voice: (617) 452-2718

Fax: (617) 253-3019

E-mail: kclee@mit.edu

ABSTRACT

In this study, new and existing methods of estimating stroke volume, cardiac output and total peripheral resistance from analysis of the arterial blood pressure waveform were tested over a wide range of conditions. These pulse contour analysis methods (PCMs) were applied to data obtained in six swine during infusion of volume, phenylephrine, dobutamine, isoproterenol, esmolol and nitroglycerine as well as during progressive hemorrhage. Performance of PCMs were compared using true end-ejection pressures as well as estimated end-ejection pressures.

There was considerable overlap in the accuracies of the PCMs when using true end-ejection measures. However, for perhaps the most clinically relevant condition, where radial artery pressure is the input, only Wesseling's Corrected Impedance method and the Kouchoukos Correction method achieved statistically superior results.

We introduced a method of estimating end-ejection by determining when the systolic pressure dropped to a value equal to the sum of the end-diastolic pressure plus a fraction of the pulse pressure. The most accurate estimation of end-ejection was obtained when that fraction was set to 60% for the central arterial pressure and to 50% for the femoral and radial arterial pressures.

When the estimated end-ejection measures were used for the PCMs that depend on end-ejection measures, when radial artery pressure was used as the input, only Wesseling's Corrected Impedance method and the modified Herd's method achieved statistically superior results.

This study provides a systematic comparison of multiple PCMs' ability to estimate stroke volume, cardiac output, and total peripheral resistance and introduces a new method of estimating end-systole.

Key words — Arterial blood pressure; cardiac output; stroke volume; total peripheral resistance; pulse contour method

INTRODUCTION

When managing patients undergoing high-risk surgeries (i.e., liver transplantation) or in the setting of an intensive care unit (ICU), monitoring cardiovascular hemodynamic information such as stroke volume (SV), cardiac output (CO), and/or total peripheral resistance (TPR) is critically important. In general, these parameters respond much more quickly to stresses (i.e., hemorrhage) than does arterial blood pressure (ABP) which is continuously controlled by multiple physiological feedback and control mechanisms to maintain a homeostatic state [1]. Thus, the ability to monitor SV or CO may enable clinical intervention at an earlier stage prior to the development of hypotension, shock, and/or organ damage during surgeries or ICU stays.

The most commonly accepted method to estimate CO in clinical settings is pulmonary artery thermodilution, which involves injecting a bolus of cold liquid through a central venous catheter into the right atrium and measuring the temperature change in the pulmonary artery [2, 3]. In general, thermodilution requires pulmonary artery catheterization, which is associated with cardiovascular risks such as carotid artery puncture (when accessing the internal jugular vein), cardiac arrhythmia, bleeding, embolism, clotting, and infection [4, 5]. Transpulmonary thermodilution has become an alternative to pulmonary artery thermodilution [6]. However, previous research has shown several limitations associated with its use [7, 8].

Even though continuous thermodilution CO measurement could provide a continuous trend of CO [9], thermodilution method cannot continuously measure SV on a beat-to-beat basis and has significant limitations [10, 11]. Therefore, many studies have thus been devoted to developing non-invasive or minimally invasive methods to continuously estimate cardiovascular parameters. These methods include Doppler ultrasound, transesophageal echocardiography, and impedance plethysomography [12-15]. However, due to various reasons, such as lack of accuracy, not providing continuous measurement, technical difficulties, requiring a medical specialist, and/or economic reasons, these systems are not popularly used and/or used only for calibration purposes in the clinical setting.

Since the arterial pulse is readily accessible, it has been commonly used to estimate the cardiovascular parameters. Specifically, mathematical analysis of the continuous ABP, termed a pulse contour method (PCM), has been extensively studied to estimate cardiovascular parameters [16-25]. However, the clinical use of this method has also been limited due to its inaccuracy.

The present study aimed to evaluate new algorithms to estimate continuous cardiovascular hemodynamic parameters. These methods were validated with measured CO using the true "gold standard for aortic blood flow (ABF) measurement method" – Transonic's ultrasonic flow probe placed on the aortic arch of the study animal – and these predictive accuracies were compared with existing PCM algorithms. In addition, for a fair comparison, a new algorithm for beat-to-beat identification of arterial end-ejection blood pressure from peripheral arteries was incorporated into the cardiovascular hemodynamic parameter estimation methods.

METHODS

The algorithms described in this section were evaluated using previously reported data (21). The following is a brief summary of the protocol. Six Yorkshire swine (30–34kg) were studied. The experimental protocol conformed to the Guide for the Care and Use of Laboratory Animals and was approved by the MIT Committee on Animal Care. The animals were pre-anesthetized with intramuscular telazol, xylazine, and atropine prior to endotracheal intubation. The swine were then maintained in a deep plane of anesthesia using inhaled anesthetic isoflurane (0.5-4 %), a mixture of oxygen and ambient air. Positive-pressure mechanical ventilation at a rate of 10-15 breathes/min, and a tidal volume of 10 ml/kg was employed.

Central ABP (CAP) was measured from the thoracic aorta using a micromanometer-tipped catheter (SPC 350, Millar Instruments, Houston, TX). Femoral ABP (FAP) and radial ABP (RAP) were measured using external fluid-filled pressure transducer (TSD104A, Biopac Systems, Santa Barbara, CA). The

chest was opened with a midline sternotomy. ABF was recoded using an ultrasonic flow probe placed around the aortic root for reference CO (T206 with A-series probes, Transonic Systems, Ithaca, NY). ABF, ECG, and ABPs were interfaced to a microcomputer via an analog-to-digital conversion system (MP150WSW, Biopac Systems, Santa Barbara, CA) at a sampling rate of 250 Hz and 16-bit resolution.

In each animal, a subset of the following interventions was performed over the course of 75 to 150 min to vary the cardiac output and other hemodynamic parameters: infusions of volume, phenylephrine, dobutamine, isoproterenol, esmolol, nitroglycerine, and progressive hemorrhage. To achieve substantial cardiac output changes in a short period (15-20 mins), several infusion rates were implemented followed by brief recovery periods (about 5 min). Also, hemorrhage was performed until a substantial change in cardiac output was observed. At the conclusion of the experiment, the animal was euthanized with the injection of sodium pentobarbital.

Algorithms

***Modified Herd's Method*:** Pulse pressure (PP) is the difference between systolic blood pressure (SBP) and diastolic blood pressure (DBP) and is regarded as a proportional measure of SV [16]. The algorithm is based on the Windkessel model with impulse ejection of SV [28]. The drawback of using PP as a proportional measure of SV is the inaccuracy introduced because of the finite duration of ejection and the distortion/alteration of the ABP waveform as it propagates through the arterial tree. In general, as the ABP waveform propagates through the tapered and bifurcated peripheral arterial branches, the SBP increases and the ABP waveform width becomes narrower.

To overcome this latter issue, Herd et al. used mean arterial pressure (MAP) instead of SBP, since MAP is less sensitive to this distortion [17]. However, when MAP is calculated by averaging the ABP waveform, the value of MAP can be affected by the duration of the diastolic interval, resulting in an SV estimation error. For example, a longer diastolic interval would result in a smaller SV estimate – even

98 though diastole follows the completion of ejection, and thus the length of diastole cannot affect the value
99 of the preceding SV. To overcome this limitation, we used mean pressure during ejection instead of mean
100 pressure averaged over the entire beat:

101 $$\frac{SV}{C_a} = \frac{1}{T_{Ejection}} \int_{Ejection} P(t)dt - DBP \qquad \textit{(Equation 1)}$$

102 C_a = arterial compliance, P = arterial blood pressure waveform, and $T_{Ejection}$ = ejection period**.** DBP is
103 the end-diastolic blood pressure of the preceding beat.

104 CO was estimated from time-averaging the SV values and TPR was calculated using the following
105 equation (Ohm's law):

106 $$MAP = CO \times TPR \qquad \textit{(Equation 2)}$$

107 CO and TPR estimates in the following methods were obtained in the same manner.

108 ***Auto-Regressive with Exogenous input (ARX) Model***: We recently introduced a novel algorithm to
109 continuously estimate beat-to-beat ABF waveforms by analysis of the ABP signal. SV can be yielded by
110 the beat-to-beat integral of the ABF waveform, and CO can be calculated by the time average of ABF
111 over number of beats in a unit time.

112 In this section, the ABF estimation method will be briefly summarized (see Ref 26 for more details).
113 The mathematical model of the system can be described as an ARX input model that relates the ABP
114 values, $P(n)$, to the ABF values, $F(n)$:

115 $$P(n) = \sum_{j=1}^{L} a(j)P(n-j) + \alpha F(n) + e(n) \qquad \textit{(Equation 3)}$$

116 where, $a(j)$ are the autoregressive coefficients, L is the parameter length, α is the weighting coefficient
117 for the exogenous input $F(n)$, and $e(n)$ is noise.

Because the input ABF is approximately zero during diastole, the autoregressive coefficients $a(j)$ can be obtained by using a least-squares method to solve Equation 3:

$$P(n_d) = \sum_{j=1}^{L} a(j)P(n_d - j) + e(n_d) \quad \textit{(Equation 4)}$$

where, n_d designates a sample point during diastole.

The coefficients $a(j)$was obtained by solving the matrix equation using Matlab (Mathworks, Natick, MA). A 17-beat moving window size was empirically found to be optimal with our algorithm for estimating the coefficients $a(j)$ and was therefore adopted. The autoregressive coefficient length was chosen to minimize $\sum a(j)$.

The exogenous input weighting coefficient (α) was obtained by taking the average of both sides of Equation 4:

$$\alpha = h\left[1 - \sum_{j=1}^{L} a(j)\right] MAP/CO \quad \textit{(Equation 5)}$$

where, MAP/CO can be obtained from Ohm's law (Equation 2).

TPR is related to the C_a and the characteristic time constant of the system (τ):

$$\tau = C_a \times TPR \quad \textit{(Equation 6)}$$

where, τ can be obtained by analyzing the terminal exponential decay curve of the impulse response of the system $h(n)$:

$$h(n) = \sum_{j=1}^{L} a(j)h(n-j) + \alpha\delta(n) \quad \textit{(Equation 7)}$$

Equations 5 and 6 can be combined to compute α:

$$\alpha = \tau\left[1 - \sum_{j=1}^{L} a(j)\right]/C_a \quad \textit{(Equation 8)}$$

Thus, instantaneous ABF can be expressed as:

$$F(n) = \frac{C_a}{\tau\left[1-\sum_{j=1}^{L} a(j)\right]}\left[P(n) - \sum_{j=1}^{L} a(j)P(n-j)\right] \quad \textit{(Equation 9)}$$

The integral of $F(n)$ was calculated on a beat-to-beat basis to obtain proportional SV estimates, and the time average of $F(n)$ over six minutes was calculated to obtain a proportional estimate of the CO (proportionality constant being C_a). Thus, the algorithm presented here provides a comprehensive set of proportional cardiovascular parameters (ABF, SV, CO, and TPR) based on an analysis of ABP waveforms.

The calculated CO, SV, and TPR using these two methods were compared with those using the previously reported methods.

Existing Pulse Contour Methods: Table 1 summarizes the existing cardiovascular parameter estimation methods that were reported to be competitive in previous comparison studies [23, 27].

Earlier works assumed that the arterial trees are represented by a two-parameter Windkessel model accounting for the total compliance of the large arteries [arterial compliance (C_a)] and the TPR of small arteries. During the diastolic period, the time constant (τ) is equal to the product of TPR and C_a and the proportional CO can be estimated using the time-averaged ABP and time constant [30]. Mukkamala et al. calculated the time constant of the Windkessel model using an autoregressive moving average analysis using arterial pressure and PP inputs to estimate the terminal projected exponential pressure decay during diastole [21].

Erlanger and Hooker described a relationship between SV and the PP suggesting that SV is proportional to the PP [16]. Meanwhile, Herd et al. used MAP instead of SBP recorded in the ascending aorta in the PP method to estimate robust SV [17]. When intra-aortic pressure is being measured continuously, it is a relatively simple matter to subtract DBP from MAP and to multiply by the heart rate (HR) to estimate CO.

Liljestrand-Zander reported that C_a varied throughout the cardiac cycle and was dependent on ABP. They used the inversely proportional relationship between C_a and ABP to correct the non-linearity [20]. Researchers also reported that SV is proportional to the area under the systolic region of the ABP waveform [18, 19, 24, 25]. Kouchoukos et al. [19] and Wesseling et al. [25] proposed an empirical and simple correction factor to the systolic area method to account for some source of error in ABP fluctuations during the systolic period. Sun et al. [23] estimated SV using the root-mean-square of the ABP waveform, which was claimed as one component of the LiDCOplus PulseCO method (LiDCO Ltd., London, England).

The aforementioned methods use information regarding end-ejection. Traditionally, researchers have used the dicrotic notch as an indicator of end-ejection**.** However, identifying the dicrotic notch can be challenging since the dicrotic notch is often not detectable, particularly in the peripheral ABP signal. For this reason, we estimated the end-systolic pressure values using the partial PP model.

Partial Pulse Pressure Model: An end-diastole always comes after a systolic peak. At end-ejection, the pressure value is less than peak SBP. One can estimate the end-ejection pressure to correspond to the ABP at the point in time when ABP falls to a value given by the following equation:

$$P_{EE} = P_{ED} + f(P_s - P_{ED}) \qquad \textit{(Equation 10)}$$

where, P_{EE}, P_{ED}, and P_S are pressure values at end-ejection, end-diastole (previous beat), and peak systole, respectively.

As examples, end-ejections identified by the 50% PP and 90% PP are shown in Figure 1. The time stamp of P_{EE} can be regarded as the time of an estimated end-ejection. To determine the accuracy of the PP model, we compared duration of diastole as estimated from the difference between the end-ejection time determined by the partial PP Model and the onset of ejection as determined from the ABP signal with the "true" duration of diastole as measured from the ABF signal. It was necessary to measure

duration of diastole because both end-ejection and onset of ejection time estimates in FAP and RAP are delayed with respect to the true times of end-ejection and onset of ejection in the ABF signal measured in the central aorta. We then determined the optimal value of the fraction *f* for each of the CAP, FAP and RAP signals. The partial PP end-ejection identification method was then applied to the PCMs for estimating SV, CO, and TPR.

The values of SV, CO, or TPR determined using the various algorithms are estimated to within a proportionality constant (determined by C_a). Therefore, the comparison of estimated to measured values of SV, CO, or TPR was achieved in each animal by adjusting the mean of each estimated parameter to match the mean of the measured value.

For all methods, end-diastolic measures were computed from the preceding cardiac cycle. The estimation errors are defined as root normalized mean squared error (RNMSE):

$$RNMSE = 100\sqrt{\sum_{n=1}^{N}[(V_{Meas} - V_{Est})/V_{Meas}]^2/(N - N_f)} \qquad \textit{(Equation 11)}$$

where, V_{Meas} and V_{Est} are the measured and estimated values (i.e., SV, CO, and TPR), respectively, N is the number of data points, and N_f is the number of free parameters.

RNMSEs of SV, CO, and TPR of each method with the true end-ejection pressure information were compared with the other methods using analysis of variance (ANOVA). In addition, RNMSEs of SV, CO, and TPR of each method with estimated end-ejection pressure using the partial PP model were compared with the other six methods using ANOVA. If a significant difference was observed, simple effects analysis with Duncan test was used to examine pair-wise differences (SAS 9.4). Statistical significance was accepted at $P<0.05$.

RESULTS

Interventions resulted in a wide range of changes of CO (1.3 – 5.8 L/min), MAP (27 – 127 mmHg), and HR (91 – 204 bpm). Table 2 summarizes the physiological ranges of the data sets. Over 68,000 beats were processed and analyzed for ABF and hemodynamic parameters. Figure 2 shows the SV, CO, and TPR estimation errors with different methods. While there was considerable overlap in the accuracies of the PCM estimates, for perhaps the most clinically relevant estimations, which use RAP as the input, only the Wesseling's Corrected Impedance and the Kouchoukos Correction methods achieved statistically superior results for all three of the estimated hemodynamic parameters.

Using the partial PP model, the end-ejection identification errors were minimum when the fraction *f* in Eq. 10 was set to 60% for CAP, 50% for FAP, and 50% for RAP - as shown in Table 3. Thus, the most accurate estimation of end-ejection was obtained when end-ejection was estimated to occur when systolic pressure dropped to a value equal to the end-diastolic pressure plus 60% (50%) of the PP for the CAP (for the FAP and RAP). Here the end-diastolic pressure and PP were referenced to the previous beat end-diastolic pressure.

In Figure 3, we show the RNSME results when using the estimated end-ejection time and pressures for methods that depend on the end-ejection measures. The above optimal values of *f* were used here. For the most clinically relevant condition where RAP is the input, only Wesseling's Corrected Impedance method and the modified Herd's method achieved statistically superior results for all three of the estimated hemodynamic parameters. In particular, Wesseling's Corrected Impedance method provided the lowest RNSMEs of 15.7% (SV), 12.3% (CO) and 12.9% (TPR).

DISCUSSION

In this paper, new algorithms were tested to estimate cardiovascular hemodynamic information. An algorithm using the ARX model to continuously estimate ABF by the analysis of peripheral ABP waveform was used to calculate CO, SV, and TPR. In addition, the modified Herd's method was tested

and systemically compared with the existing hemodynamic parameter estimation methods using the same ABP dataset. We also tested existing PCM algorithms and evaluated the impact of estimating end-ejection time and pressure on the performance of the PCM algorithms.

There was considerable overlap in the accuracies of the PCM estimates when using true end-ejection pressures. However, for perhaps the most clinically relevant estimations, which use radial artery pressure as the input, only the Wesseling's Corrected Impedance and the Kouchoukos Correction methods achieved statistically superior results for all three of the estimated hemodynamic parameters.

All the methods incorporate their own assumptions in cardiovascular physiology. Cardiovascular hemodynamic parameter estimation methods need to work under a wide set of physiological conditions in clinical and research settings. The parameters of Wesseling's Corrected Impedance method [25] were empirically obtained from a human study. In this method, the systolic area under the ABP curve above DBP was scaled using a scaling factor that is a function of HR and MAP. Although the scaling factor formula was obtained from healthy male subjects in their twenties, the method achieved low errors when applied to the swine data sets, indicating that the human and swine cardiovascular system may be similar in terms of applicability of the model. The Kouchoukos Correction method [19] includes a simple correction factor (T_S/T_D) to model run-off blood flow during systole. Although the correction factors are in both cases empirical, the Wesseling's and Kouchoukos's methods achieved lower errors than several theoretical model-based methods.

Liljestrand-Zander's method [20] unexpectedly generated high errors with the swine data, although it has been reported to have the best agreement with the thermodilution CO in ICU patient data sets [23]. This could be attributed to the nature of the ICU data sets. Because clinicians attempt to maintain the patient's ABP and CO, there is less variation in these signals obtained from patients than those obtained during animal experiments in which these signals can be varied more widely using a variety of interventions. Thus, methods that tend to provide stable estimates may appear to perform better with

patient data where the majority of the input parameters are stable. However, the utility of a method to measure CO and other cardiac hemodynamic parameters is to identify those rare occasions when these parameters deviate substantially from their normal values. The data analysis employed in this study was designed to weigh the tail values specifically to test this aspect.

For the hemodynamic parameter estimation, end-systole (onset of diastole) needs to be determined for each beat. In practical settings, a standard method to detect the end-systole (onset of diastole) is the use of the dicrotic notch in ABP waveforms. However, the dicrotic notch does not always exist in the ABP waveform. Therefore, we evaluated the performance of a model to estimate end-ejection (Eq. 10).

The most accurate estimation of end-ejection was obtained when end-ejection was estimated to occur when systolic pressure dropped to a value equal to the end-diastolic pressure plus 60% (50%) of the PP for the CAP (for the FAP and RAP). Here the end-diastolic pressure and PP are referenced to the previous beat end-diastolic pressure.

In Figure 3, we show the RNSME results when using the estimated end-ejection pressures for methods that depend on the end-ejection pressure. Here, for the most clinically relevant condition when radial artery pressure is the input, only Wesseling's Corrected Impedance method and the modified Herd's method achieved statistically superior results for all three of the estimated hemodynamic parameters. In particular, Wesseling's Corrected Impedance method provided the lowest RNSMEs.

The ARX algorithm utilizes the notion that the input to the arterial system is zero during diastole. In the ABF estimation routine, 17 diastolic ABP waveforms were used to obtain the autoregressive (AR) parameter and the AR parameters were integrated into the ARX model and applied to the entire ABP waveform to obtain the ABF waveform. The AR parameters were also used to obtain the characteristic time constant as well as the scaling factor to properly scale the estimated ABF. The 17-beat moving window size was empirically chosen. If the window is too short, one cannot excite enough modes to identify the system. On the other hand, if the window is too long, one cannot assume time-invariance of

the pertinent cardiovascular system. This method provides not only proportional SV, CO, and TPR, but also instantaneous ABF waveforms without training data sets or demographic hemodynamic parameters - arguably one of the most comprehensive estimation algorithms to our knowledge.

The classical Windkessel model assumes exponential decay during diastole and this model can be described as a low-order AR model. The present ARX algorithm, on the other hand, obtains higher-order AR parameter from diastolic ABP waveforms. The advantage of the present ARX algorithm is that it appears to take into account possible distortion in the diastolic ABP waveforms in that the filter created by the algorithm can reliably reconstruct the systolic ABF waveform. The distortion property may vary from artery to artery, as well as from subject to subject. The algorithm could obtain individual parameters unique to each arterial line of each subject on a beat-to-beat basis.

Further development of accurate end-systole identification methods (e.g., perhaps incorporating heart sounds) might lead to more robust SV, CO, and TPR estimation using the new methods. Future work is needed to apply and validate the algorithm with abnormal beats, such as premature beats and in heart failure models. The methods could also be applied to optimizing SV when programming atrioventricular time delay for conventional pacemakers and timing parameters for biventricular pacing.

One limitation of the current work is that the animal data involved using healthy pigs (~35 kg) with normal hearts. Further studies would be necessary to apply the methods described here under a variety of pathological clinical conditions (e.g. heart failure). The methods described here also need to be evaluated using human data under various clinical conditions and populations.

CONCLUSION

297 This paper tested new algorithms to estimate hemodynamic parameters (SV, CO, and TPR) by
298 analysis of the ABP signal. Additionally, a new algorithm to identify end-ejection was implemented in
299 conventional and the new hemodynamic parameter estimation algorithms.

300 There was considerable overlap in the accuracies of the PCM estimates when using true end-ejection
301 pressures. However, for perhaps the most clinically relevant estimations, which use radial artery pressure
302 as the input, only the Wesseling's Corrected Impedance and the Kouchoukos Correction methods
303 achieved statistically superior results for all three of the estimated hemodynamic parameters.

304 The Wesseling's Corrected Impedance method and the modified Herd's method performed best
305 among methods that depended on end-ejection time or pressure when estimated, rather than true, values
306 of end-ejection measures were used. In particular, the Wesseling's Corrected Impedance method
307 provided the lowest errors.

308

Compliance with ethical standards

Conflict of Interest Richard Cohen is a co-inventor on two patents in the area of hemodynamic parameter estimation assigned to the Massachusetts Institute of Technology (MIT) which have been licensed to Retia Medical, LLC. Dr. Cohen is not otherwise involved with the company. The other authors declare no conflicts.

Ethical approval All procedures performed in studies involving animals were in accordance with the ethical standards of the institution.

REFERENCES

[1] H. Barcroft, O.G. Edholm, J. McMichael, and E.P. Sharpey-Schafer, "Posthaemorrhagic fainting. Study by cardiac output and forearm flow," Lancet, vol. 1, pp. 489-491, 1944.

[2] W. Ganz, R. Donoso, H.S. Marcus, J.S. Forrester, and H.J. Swan, "A new technique for measurement of cardiac output by thermodilution in man," Am J Cardiol, vol. 27, pp. 392-6, 1971.

[3] W. Ganz and H.J. Swan, "Measurement of blood flow by thermodilution," Am J Cardiol, vol. 29, pp. 241-6, 1972.

[4] G.R. Manecke, Jr., J.C. Brown, A.A. Landau, D.P. Kapelanski, C.M. St Laurent, and W.R. Auger, "An unusual case of pulmonary artery catheter malfunction," Anesth Analg, vol. 95, pp. 302-4, 2002.

[5] J.S. Vender and H.C. Gilbert, “Monitoring the anesthetized patient,” 3 ed. Philadelphia: Lippincott-Raven Publishers, 1997.

[6] X. Monnet and J.L. Teboul, “Transpulmonary thermodilution: advantages and limits,” Crit Care, vol. 21, pp. 147, 2017.

[7] L. Huter, K.R. Schwarzkopf, N.P. Schubert, and T. Schreiber, “The level of cardiac output affects the relationship and agreement between pulmonary artery and transpulmonary aortic thermodilution measurements in an animal model,” J Cardiotheorac Vasc Anesth, vol. 21, pp. 659-63, 2007.

[8] K. Staier, M. Wilhelm, C. Wiesenack, M. Thoma, and C. Keyl, “Pulmonary artery vs. transpulmonary thermodilution for the assessment of cardiac output in mitral regurgitation: a prospective observational study,” Eur J Anaesthesiol, vol. 29, pp. 431-7, 2012.

[9] F.G. Mihm, A. Gettinger, C.W. Hanson, 3rd, H.C. Gilbert, E.P. Stover, J.S. Vender, B. Beerle, and G. Haddow, "A multicenter evaluation of a new continuous cardiac output pulmonary artery catheter system," Crit Care Med, vol. 26, pp. 1346-50, 1998.

[10] M. Botero, D. Kirby, E.B. Lobato, E.D. Staples, and N. Gravenstein, "Measurement of cardiac output before and after cardiopulmonary bypass: Comparison among aortic transit-time ultrasound, thermodilution, and noninvasive partial CO2 rebreathing," J Cardiothorac Vasc Anesth, vol. 18, pp. 563-72, 2004.

[11] W.H. Fares, S.K. Blanchard, G.A. Stouffer, P.P. Chang, W.D. Rosamond, H.J. Ford, and R.M. Aris, "Thermodilution and Fick cardiac outputs differ: impact on pulmonary hypertension evaluation," Can Respir J, vol. 19, pp. 261-6, 2012.

[12] M.E. Blohm, D. Obrecht, J. Hartwich, G.C. Mueller, J.F. Kersten, J. Weil, and D. Singer, "Impedance cardiography (electrical velocimetry) and transthoracic echocardiography for non-invasive cardiac output monitoring in pediatric intensive care patients: a prospective single-center observational study," Crit Care, vol. 18, pp. 603, 2014.

[13] S. Schubert, T. Schmitz, M. Weiss, N. Nagdyman, M. Huebler, V. Alexi-Meskishvili, F. Berger, and B. Stiller, "Continuous, non-invasive techniques to determine cardiac output in children after cardiac surgery: evaluation of transesophageal Doppler and electric velocimetry," J Clin Monit Comput, vol. 22, pp. 299-307, 2008.

[14] S. Scolletta, F. Franchi, S. Romagnoli, R. Carla, A. Donati, L.P. Fabbri, F. Forfori, J.M. Alonso-Inigo, S. Laviola, V. Mangani, G. Maj, G. Martinelli, L. Mirabella, A. Morelli, P. Persona, D. Payen, and PulseCOval Group, "Comparison Between Doppler-Echocardiography and Uncalibrated Pulse Contour Method for Cardiac Output Measurement: A Multicenter Observational Study," Crit Care Med, vol. 44, pp. 1370-9, 2016.

[15] R.P. Patterson, "Fundamentals of impedance cardiography," IEEE Eng Med Biol Mag, vol. 8, pp. 35-8, 1989.

[16] J. Erlanger and D.R. Hooker, "An experimental study of blood-pressure and of pulse-pressure in man," Johns Hopkins Hosp Rep, vol. 12, pp. 145-378, 1904.

[17] J.A. Herd, N.R. Leclair, and W. Simon, "Arterial pressure pulse contours during hemorrhage in anesthetized dogs," J Appl Physiol, vol. 21, pp. 1864-8, 1966.

[18] W.B. Jones, L.L. Hefner, W.H. Bancroft, Jr., and W. Klip, "Velocity of blood flow and stroke volume obtained from the pressure pulse," J Clin Invest, vol. 38, pp. 2087-90, 1959.

[19] N.T. Kouchoukos, L.C. Sheppard, and D.A. McDonald, "Estimation of stroke volume in the dog by a pulse contour method," Circ Res, vol. 26, pp. 611-23, 1970.

[20] G. Liljestrand and E. Zander, "Vergleichende Bestimmung des Minutenvolumens des Herzens beim Menschen mittels der Stickoxydulmethode und durch Blutdruckmessung," Zeitschrift fur die gesamte experimentelle Medizin, vol. 59, pp. 105-122, 1928.

[21] R. Mukkamala, A.T. Reisner, H.M. Hojman, R.G. Mark, and R.J. Cohen, "Continuous cardiac output monitoring by peripheral blood pressure waveform analysis," IEEE Trans Biomed Eng, vol. 53, pp. 459-67, 2006.

[22] T. Parlikar, T. Heldt, G.V. Ranade, and G. Verghese, "Model-Based Estimation of Cardiac Output and Total Peripheral Resistance," presented at the Computers in Cardiology, pp. 379-82, 2007.

[23] J.X. Sun, A.T. Reisner, M. Saeed, T. Heldt, and R.G. Mark, "The cardiac output from blood pressure algorithms trial," Crit Care Med, vol. 37, pp. 72-80, 2009.

[24] P.D. Verdouw, J. Beaune, J. Roelandt, and P.G. Hugenholtz, "Stroke volume from central aortic pressure? A critical assessment of the various formulae as to their clinical value," Basic Res Cardiol, vol. 70, pp. 377-89, 1975.

[25] K.H. Wesseling, B. De Werr, J.A.P. Weber, and N.T. Smith, "A simple device for the continuous measurement of cardiac output. Its model basis and experimental verification," Adv Cardiovasc Phys, vol. 5, pp. 16-52, 1983.

[26] T. Arai, K. Lee, R.P. Marini, and R.J. Cohen, "Estimation of changes in instantaneous aortic blood flow by the analysis of arterial blood pressure," J Appl Physiol, vol. 112, pp. 1832-8, 2012.

[27] T. Parlikar, "Modeling and Monitoring of Cardiovascular Dynamics for Patients in Critical Care," Department of Electrical Engineering and Computer Science, Massachusetts Institute of Technology, Cambridge, 2007.

[28] M.J. Bourgeois, B.K. Gilbert, G. Von Bernuth, and E.H. Wood, "Continuous determination of beat to beat stroke volume from aortic pulse pressures in the dog," Circ Res, vol. 39, pp. 15-24, 1976.

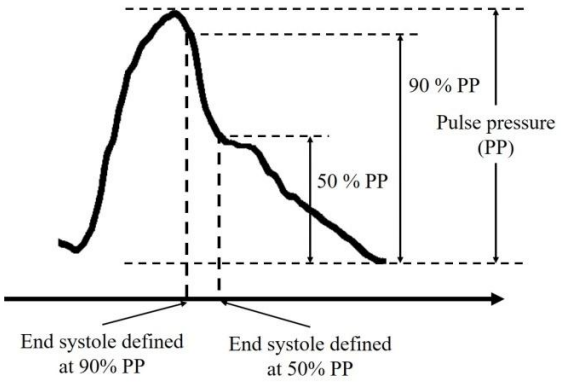

403 Fig 1. End-systole (ejection) defined by means of the partial pulse pressure (PP). 50% and 90 % PP are
404 shown as examples.

405

406

407

408

409

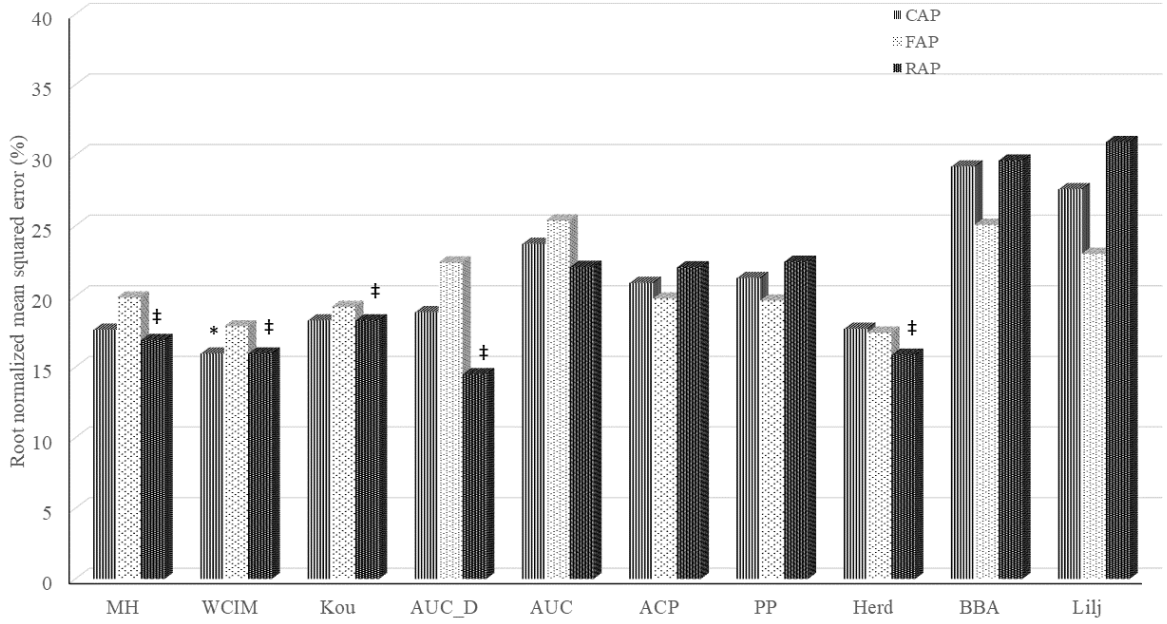

410

411 a) SV

412

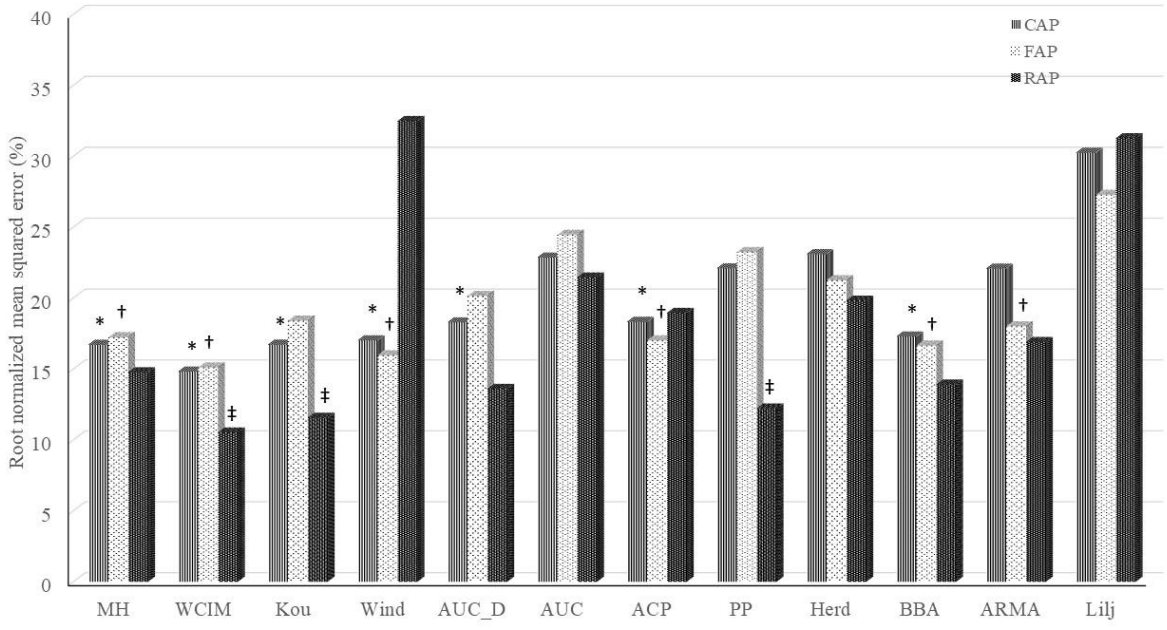

413

414 b) CO

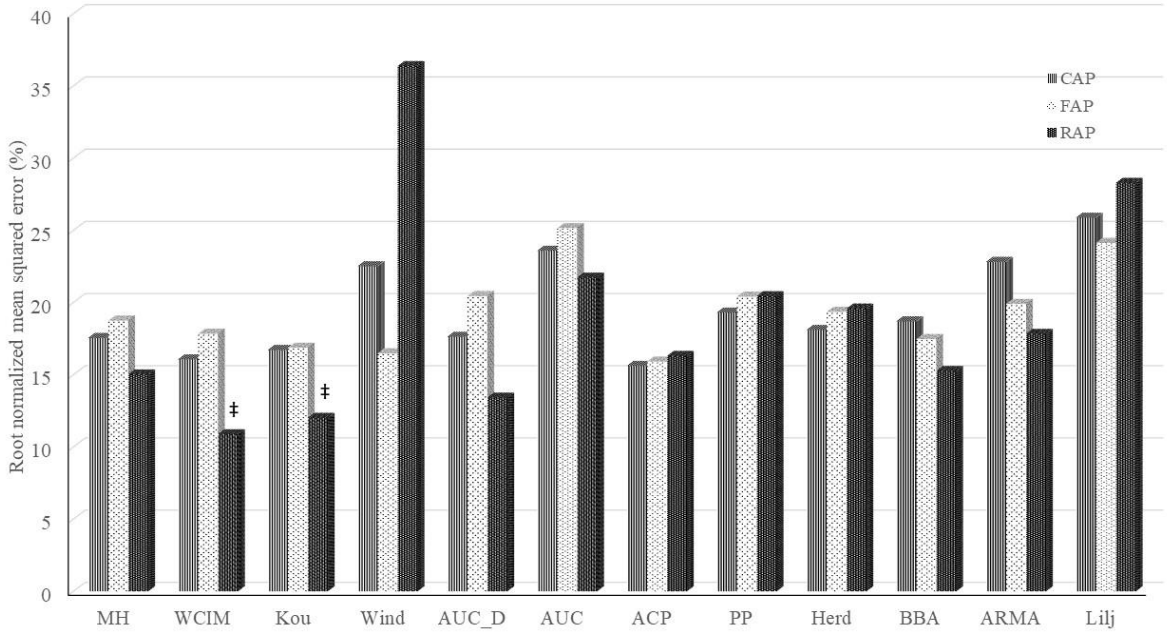

c) TPR

Figure 2. The SV, CO, and TPR estimation errors with different methods using the measured end-ejection pressure.

* P<0.05 lower than other methods with central arterial pressure (CAP). † P<0.05 lower than other methods with femoral arterial pressure (FAP). ‡ P<0.05 lower than other methods with radial arterial pressure (RAP)

MH: modified Herd's method; WCIM: Wesseling's corrected impedance method; Kou: Kouchoukos correction; Wind: Windkessel model AUC_D: area under the curve with end-diastolic ABP value subtracted; AUC: area under the systolic curve; ACP: alternating current power; PP: pulse pressure; Herd: Herd's pulse pressure; BBA: beat-to-beat average; ARMA: autoregressive moving average; Lilj: Liljestrand-Zander's.

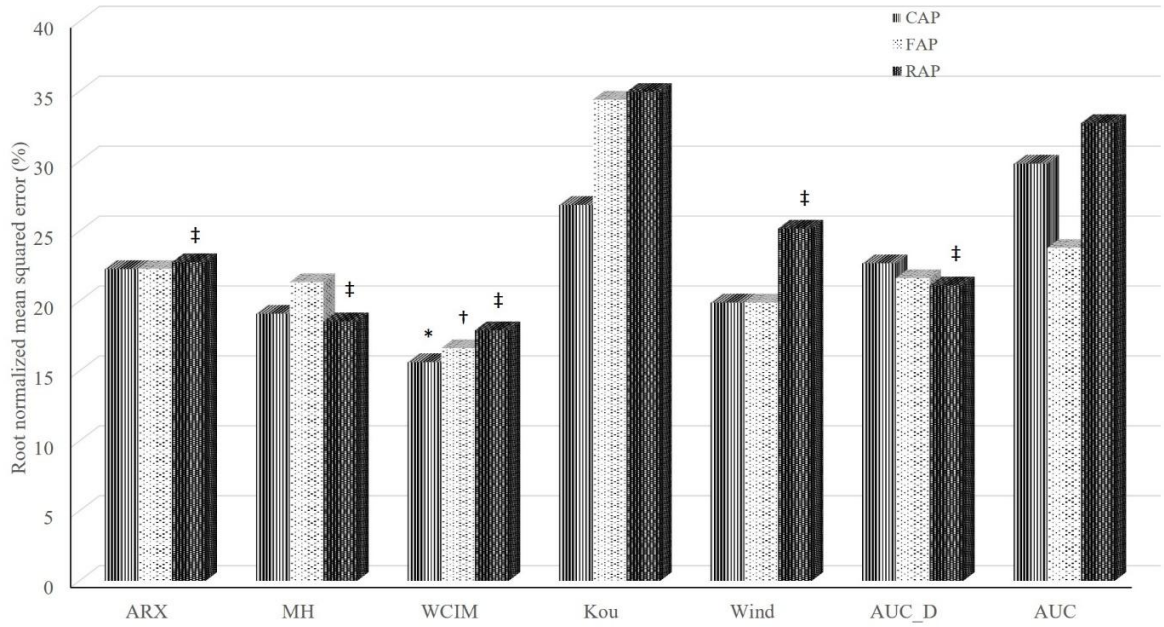

a) SV

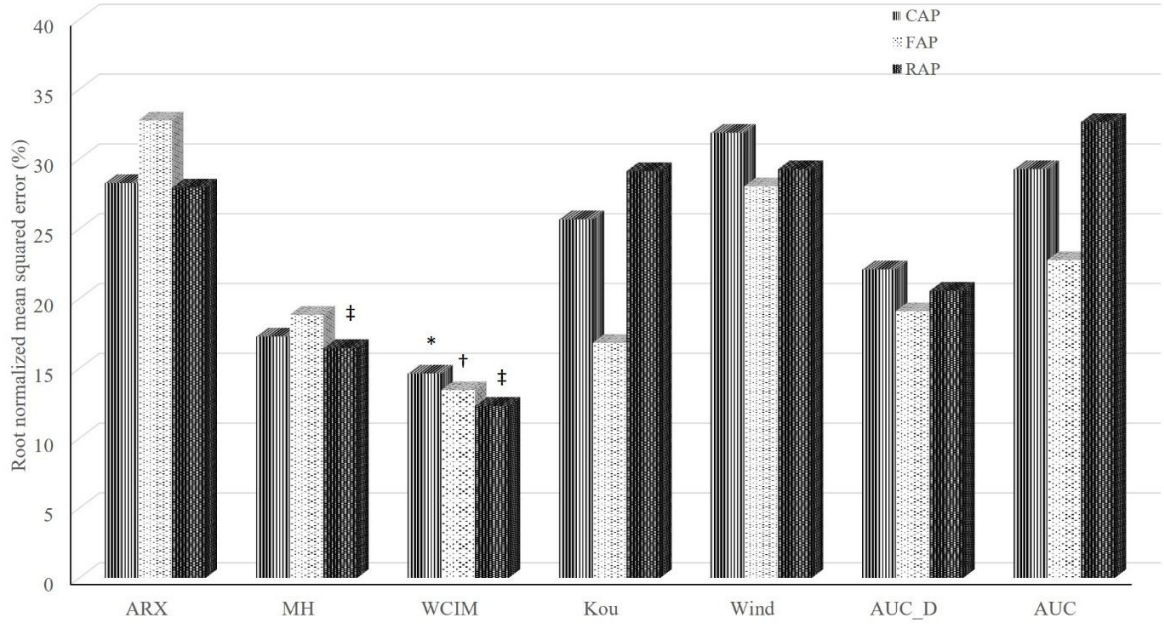

b) CO

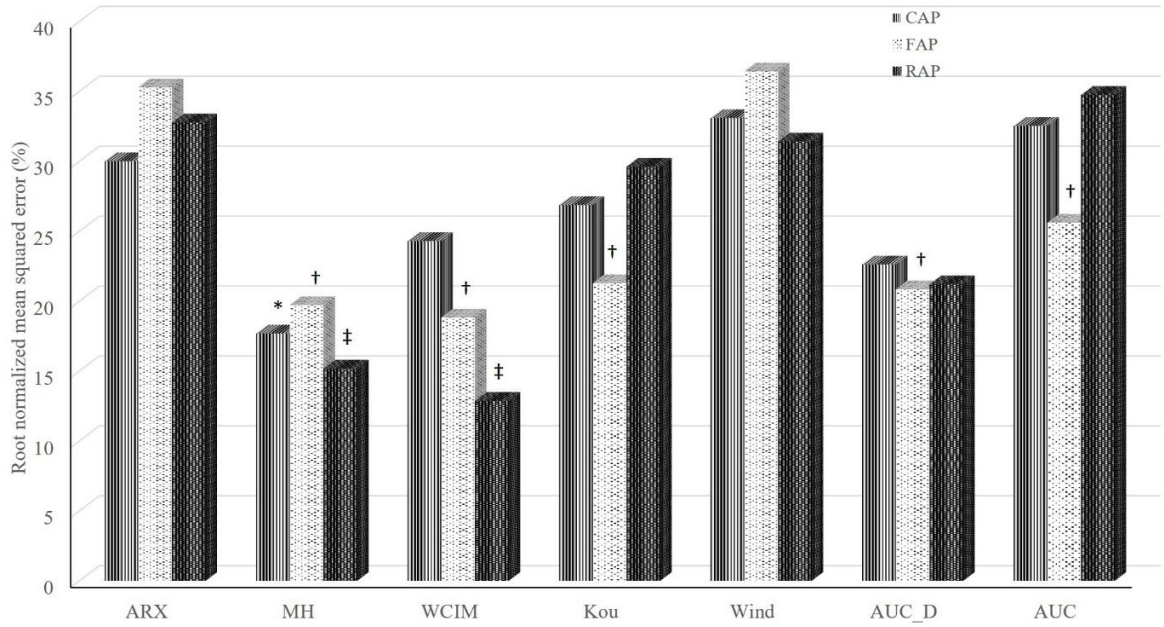

c) TPR

Figure 3. The SV, CO, and TPR estimation errors with different methods using the partial pulse pressure model to estimate end-ejection pressure.

* P<0.05 lower than other methods with central arterial pressure (CAP). † P<0.05 lower than other methods with femoral arterial pressure (FAP). ‡ P<0.05 lower than other methods with radial arterial pressure (RAP)

ARX, ARX model with exogenous input; MH: modified Herd's method; WCIM: Wesseling's corrected impedance method; Kou: Kouchoukos correction; Wind: Windkessel model AUC_D: area under the curve with end-diastolic ABP value subtracted; AUC: area under the systolic curve.

449 Table 1. Existing cardiovascular hemodynamic parameter estimation methods.

450

Windkessel Model [28]	$\tau = TPR \cdot C_a \quad CO \propto \frac{MAP}{\tau}, \quad \frac{F}{C_a} = \frac{dP}{dt} + \frac{P}{\tau}$
Pulse Pressure [16]	$SV \propto PP = SBP - DBP$
Herd's Pulse Pressure [17]	$SV \propto MAP - DBP$
Liljestrand-Zander's [20]	$SV = C_a \times PP \propto \frac{SBP - DBP}{SBP + DBP}$
Beat-to-Beat Average (BBA) Model [22]	$CO \propto \frac{P_2 - P_1}{T} + \frac{MAP}{\tau}$
Systolic Area [18], [24]	$SV \propto \int_{t^{ED}}^{t^{EE}} P(t)dt \quad or \quad SV \propto \int_{t^{ED}}^{t^{EE}} (P(t) - DBP)dt$
Wesseling's Corrected Impedance [25]	$SV \propto (163 + HR - 0.48 \cdot MAP) \int_{t^{ED}}^{t^{EE}} (P(t) - DBP)dt$
Kouchoukos Correction [19]	$SV \propto \left(1 + \frac{T_S}{T_D}\right) \int_{t^{ED}}^{t^{EE}} (P(t) - DBP)dt$
Alternating Current Power [23]	$SV \propto \sqrt{\frac{1}{T}\int_T (P(t) - MAP)^2 dt}$
Auto-Regressive Moving Average [21]	$P[i] = \sum_{j=1}^{p} a[j]P[i-j] + \sum_{k=1}^{q} b[k]PP[i-k]$ $CO = \frac{MAP}{TPR} \propto \frac{MAP}{\tau}$

PP: pulse pressure; SBP: systolic blood pressure; DBP: diastolic blood pressure; MAP: mean arterial pressure; C_a: compliance of the arterial tree; CO: cardiac output; SV: stroke volume; **F: aortic blood flow;** T: duration of cardiac cycle; P_1: arterial blood pressure at the beginning of the beat; P_2: arterial blood pressure at the end of the beat; τ: time constant of arterial system; P: arterial blood pressure; t: time; HR: heart rate; T_S: systolic duration in Kouchoukos correction method; T_D: diastolic duration in Kouchoukos method; t^{ED}: time at which end-diastole occurs; **t^{EE}: time at which** end-ejection **occurs;** $a[j]$: autoregression coefficients; $b[k]$: moving average coefficients; TPR: total peripheral resistance.

461 **Table 2. Summary of hemodynamic parameters (Mean ± SD) of the six swine data sets.**

	CO (L/min)	SV (mL)	FAP (mmHg)	RAP (mmHg)	HR (bpm)
1	3.6±1.0	28.4±5.8	63±19	61±19	129±29
2	3.2±0.6	25.0±5.0	83±21	73±20	135±38
3	4.0±0.7	31.7±7.1	83±16	87±15	133±32
4	3.2±0.6	25.2±4.3	89±19	79±18	129±34
5	3.3±0.5	26.7±6.4	80±21	85±29	130±32
6	3.4±1.2	28.5±8.1	72±19	75±20	130±26
Mean	3.5±0.8	27.5±6.7	79±21	76±21	131±32

462

463

464 CO: cardiac output, SV: stroke volume, FAP: femoral arterial pressure, RAP: radial arterial pressure, HR:
465 heart rate.

466

467 Table 3. Summary of diastolic interval error ± SD (%).

468

	CAP	FAP	RAP
40% PP	17.1 ± 11.6	5.9 ± 8.0	6.0 ± 14.2
50% PP	10.1 ± 9.0	-3.3 ± 5.5	-1.4 ± 12.5
60% PP	1.8 ± 6.9	-7.4 ± 4.1	-10.8 ± 6.8
70% PP	-4.7 ± 4.3	-10.0 ± 3.9	-13.8 ± 7.1
80% PP	-8.2 ± 3.5	-12.8 ± 3.9	-17.1 ± 8.2
90% PP	-11.3 ± 3.8	-16.3 ± 4.3	-23.8 ± 11.3

469

470 PP: pulse pressure, CAP: central arterial pressure, FAP: femoral arterial pressure, RAP: radial arterial
471 pressure.

472

GLOSSARY:

ABF: aortic blood flow

ABP: arterial blood pressure

ACP: alternating current power

AR: autoregressive

ARMA: autoregressive moving-average model

ARX: autoregressive with exogenous input

AUC: area under the systolic

AUC_D: Area under the curve with end-diastolic ABP value subtracted

BBA: beat-to-beat averaged model

C_a: arterial compliance

CAP: central arterial pressure

CO: cardiac output

DBP: diastolic blood pressure

FAP: femoral arterial pressure

HR: heart rate

ICU: intensive care unit

MAP: mean arterial pressure

MH: modified Herd's method

PCM: pulse contour method

PP: Pulse pressure

RAP: radial arterial pressure

RNMSE: root normalized mean squared error

SBP: systolic blood pressure

SV: stroke volume

TPR: total peripheral resistance

WCIM: Wesseling's corrected impedance method